Treatment Site Uncertainties in IGRT

Krishni Wijesooriya, PhD
University of Virginia

University of Virginia Health System

Department of Radiation Oncology

Outline

- Image registration accuracies for different modalities
  - What imaging modality best suited for each site?
  - What imaging modality best suited for each Tx type?
- For each site, will discuss
  - Site-specific goals and uncertainties
  - Dosimetric consequences of exceeding tolerances
  - Desirable IGRT characteristics and feasible systems to achieve goals
  - IGRT process designs to minimize site-specific uncertainties
  - Sites used as examples of critical thinking process in this presentation: lung, liver, prostate, spine SBRT, H&N
- Offline and on-line correction strategies
  - Differences
  - Importance of time and efficiency of verification.
  - How to use them and when to use them

- Image registration accuracies for different modalities
  - What imaging modality best suited for each site?
  - What imaging modality best suited for each Tx type ?

Executive summary of AAPM/ASTRO on image guided technologies

International Journal of Radiation Oncology biology ● physics

www.redjournal.org

Critical Review

Image Guided Radiation Therapy (IGRT) Technologies for Radiation Therapy Localization and Delivery

Jennifer De Los Santos, MD,* Richard Popple, PhD,* Nzhde Agazaryan, PhD,† John E. Bayouth, PhD,‡ Jean-Pierre Bissonnette, PhD,§ Mary Kara Bucci, MD,‖ Sonja Dieterich, PhD,¶ Lei Dong, PhD,# Kenneth M. Forster, PhD,** Daniel Indelicato, MD,†† Katja Langen, PhD,‡‡ Joerg Lehmann, PhD,¶ Nina Mayr, MD,§§ Ishmael Parsai, PhD,¶¶ William Salter, PhD,## Michael Tomblyn, MD, MS,*** William T.C. Yuh, MD, MSEE,‖‖ and Indrin J. Chetty, PhD†††

*Department of Radiation Oncology, University of Alabama at Birmingham, Birmingham, Alabama; †Department of Radiation Oncology, University of California Los Angeles, Los Angeles, California; ‡Department of Radiation Oncology, University of Iowa, Iowa City, Iowa; §Department of Radiation Physics, Princess Margaret Hospital, Toronto, Ontario, Canada; ‖Anchorage Radiation Therapy Center, Anchorage, Alaska; ¶Department of Radiation Oncology, University of California Davis, Sacramento, California; #Scripps Proton Therapy Center, San Diego, California; **Department of Radiation Oncology, University of South Alabama, Mobile, Alabama; ††Department of Radiation Oncology, University of Florida Proton Therapy Institute, Jacksonville, Florida; ‡‡Department of Radiation Oncology, MD Anderson Cancer Center Orlando, Orlando, Florida; Departments of §§Radiation Oncology and ‖‖Radiology, Ohio State University, Columbus, Ohio; ¶¶Department of Radiation Oncology, University of Toledo College of Medicine, Toledo, Ohio; ##Department of Radiation Oncology, Huntsman Cancer Hospital, Salt Lake City, Utah; ***Department of Radiation Oncology, Moffitt Cancer Center, Tampa, Florida; and †††Department of Radiation Oncology, Henry Ford Hospital and Health Centers, Detroit, Michigan

Received Sep 6, 2012, and in revised form Feb 14, 2013. Accepted for publication Feb 16, 2013

IGRT modalities, accuracies, and sites –Radiation Based systems

Table 1 Radiation-based systems for IGRT / **Table 1** *(continued)*

Radiation-based systems		Imaging acquisition	Average dose per image*	Geometric accuracy	Functionality and routine clinical use	Examples of sites where technology has been commonly applied	Benefits and caveats
Electronic portal imaging devices (EPIDs)	Examples						
kV or MV 2-D planar	Varian, Siemens, Elekta	2-D	1-3 mGy	1-2 mm	MV or kV "snapshot" planar images; used to acquire portal images for verification of setup based on bony landmarks	Prostate/pelvis Head and neck Lung/thorax Breast Pelvis/gynecologic tumors	Appropriate if bony landmarks serve as a good surrogate for tumor localization; does not acquire 3-D, volumetric information, and is static; kV x-rays will offer better image contrast than MV; kV x-rays will suffer from artifacts in the presence of high-density structures, such as hip prostheses
Stereoscopic kV imaging	Accuracy (Cyberknife)	2-D	0.10-200 mGy	<1 mm	kV-pretreatment planar images and images during treatment to track motion; alignment performed based on implanted markers or marker or bony landmarks; robotic positioning accounts for "6-D," translational and rotational setup corrections	Prostate/pelvis Lung/thorax Gynecologic tumors Brain SBRT/SRS	Appropriate if bony landmarks serve as a good surrogate for tumor localization; does not acquire 3-D, volumetric information
	BrainLAB (Novalis)	2-D	0.33-0.55 mGy	<1 mm	An optical guidance system in conjunction with stereoscopic, planar kV images and "snapshot" images during treatment to detect patient motion; used for bony alignment and to compensate for patient motion during treatment; uses a "6-D" treatment couch to compensate for translational and rotational setup corrections	SBRT/SRS Brain Spine Lung Liver Head and neck Gynecologic tumors	Appropriate if bony landmarks serve as a good surrogate for target localization; does not acquire 3-D, volumetric information, and is static. "Snapshot" imaging evaluates movement of bony landmarks during treatment, and subsequent termination of the beam and realignment of the patient, if necessary
	BrainLAB/MHI (VERO)	2-D	0.33-0.55 mGy	0.1 mm	A pair of x-rays and couch motion used for initial alignment; for patient motion during treatment; subsequently, the on-board imaging system acquires x-rays and correction of "6-D" setup errors is performed by translating and rotating the x-ray, mounted on gimbals		Appropriate if bony landmarks serve as a good surrogate for target localization; includes volumetric data acquisition (see CBCT section)
Cone-beam CT (CBCT)	Examples						
	Varian, Elekta, Siemens, BrainLab (VERO)	3-D	30-50 mGy	≤1 mm	kV or MV cone beam CT (CBCT); localization based on volumetric image acquisition and 3-D–3-D matching with treatment planning CT; for the x-ray source/detector arms for CBCT, volumetric CBCT data acquisition is performed by rotating the O-ring (x-ray source) and the flat panel detector 200°	SBRT/SRS Lung/thorax Liver Brain Head and neck Spine	Is a slow scan, which tends to acquire the "average" position of organs undergoing respiratory-induced motion; can be used for monitoring patient setup (interfraction motion) and changes in anatomy that have occurred possibly during treatment, by performing imaging immediately after treatment; has the ability to monitor tumor response through course of therapy; kV CBCT has better contrast resolution than MV CBCT; kV CBCT suffers from artifacts in the presence of high density materials (eg, hip prostheses); patient scatter (especially for larger patients) can degrade image quality for kV CBCT
CT-on-rails	Examples Siemens CT-on-rails	3-D	10-50 mGy	≤1 mm	Fan-beam kV CT; used for routine volumetric imaging to ensure accurate targeting of the radiation \beam	Prostate Head and neck Lung/thorax Paraspinal tumors	Can be used for monitoring patient setup (interfraction motion) and changes in anatomy that have occurred possibly during treatment, by performing imaging immediately after treatment; has the ability to monitor tumor response through the course of therapy
MVCT	Examples Tomotherapy	3-D	10-30 mGy	≤1 mm	Fan-beam MV CT; used for routine volumetric imaging to ensure accurate targeting of the radiation beam	Prostate Lung/thorax Breast Gynecologic tumors Head and neck Paraspinal tumors Esophagus Sarcomas GI malignancies	Has the ability to monitor tumor response through course of therapy

IGRT modalities, accuracies, and sites –Non Radiation based systems

38 De Los Santos et al. International Journal of Radiation Oncology • Biology • Physics

Table 2 Non-radiation-based systems for IGRT

Non-radiation-based systems		Imaging acquisition	Geometric accuracy	Functionality/ technical abilities
Ultrasound	Examples BAT, SonArray, iBEAM, RESTITU/Clarity	3-D	3-5 mm	Used for ultrasound-based alignment of target to decrease interfraction setup errors
Camera-based	Examples AlignRT	3-D	1-2 mm	Used for surface-based localization
Magnetic resonance imaging	Examples Viewray	3-D	1-2 mm	Used for localization based on MRI
Non-x-ray 4-D tracking systems Electromagnetic	Examples Calypso	<2 mm	System is independent from the linac	Electromagnetic transponders implanted in the prostate gland, used for improving setup accuracy and for accounting for intrafraction motion of the prostate gland

Volume 87 • Number 1 • 2013 IGRT for localization and treatment delivery 39

Table 2 *(continued)*

Non-radiation-based systems	Examples of sites where technology has been commonly applied	Benefits and caveats
Ultrasound	Prostate Lung	Nonionizing; real-time assessment of intrafraction motion will soon be possible with 4-D ultrasound; potential higher interuser variability
Camera-based	Breast Prostate Respiratory gating	Appropriate if the surface serves as a good surrogate for localization of the target; gating is also possible based on respiratory monitoring of an external surrogate
Magnetic resonance imaging	Prostate Hepatocellular carcinoma Brachytherapy Brain	Enhanced visualization of soft tissue without the need for ionizing radiation MRI is confounded by distortion resulting from nonuniformity in the magnetic field, magnetic susceptibility artifacts, patient motion, etc.
Non-x-ray 4-D tracking systems Electromagnetic	Prostate	Real-time assessment of intrafraction motion of the prostate gland; radiation beam can be halted if transponder motion is outside a predefined tolerance, thereby improving localization accuracy in "real time"; implantation of transponders in the prostate is considered invasive; location of the transponder readout array limits applicability based on the size of the patient; transponders cause artifacts on MR images

Executive summary of AAPM/ASTRO on image guided technologies

J. De Los Santos et al. " Iimage guided radiation therapy (IGRT) technologies for radiation therapy localization and delivery" IJROBP 87(1) 33-45; 2013

IGRT modalities, accuracies, and sites – 4D systems

Radiation-based systems		Imaging acquisition	Average dose per image*	Geometric accuracy	Functionality and routine clinical use	Examples of sites where technology has been commonly applied	Benefits and caveats
X-ray real-time tracking systems	Examples						
Combined infrared and 2-D orthogonal kV imaging localization	BrainLAB (ExacTrac)	4-D		An optical, infrared camera system, along with 2 x-ray imagers located obliquely in the treatment room for stereoscopic imaging	Tumor tracking, using x-ray images and based on correlation between tumor position and external markers, updated during treatment using kV orthogonal imaging	SBRT/SRS Brain Spine Lung Liver Head and neck Gynecologic tumors	Correlation between external markers and internal tumor motion helps circumvent possible phase offsets; implantation of markers, if required, is an invasive procedure
	Accuray (CyberKnife)	4-D		A robot capable of movement around the patient except from angles posterior to the couch	Tumor tracking, using x-ray images and based on correlation between tumor position and external markers using an adaptive model, updated during treatment using kV orthogonal imaging	SBRT/SRS Brain Spine Lung Liver	Correlation between external markers and internal tumor motion helps circumvent possible phase offsets; implantation of markers, if required, is an invasive procedure
	BrainLAB/MHI (VERO)	4-D			Tumor motion compensation performed by fluoroscopic imaging during treatment, target delineation on the images, and tracking of the center of mass of the target		Target delineation on fluoroscopic images is confounded by lack of soft-tissue contrast
	RTRT (Hokkaido, Mitsubishi)	4-D	0.20-20 mGy Estimated skin dose from 1 fluoroscope: 29-1182 mGy/h	<1 mm static accuracy; <1.5 mm for a target moving up to 40 mm/s	Implanted artificial fiducials are located and continuously tracked by 2 of the 4 orthogonal imaging systems during treatment	Lung Liver Prostate Spinal tumors	Real-time imaging of implanted fiducials can result in very high skin doses, up to 1200 mGy/h from 1 fluoroscopic procedure of the

Executive summary of AAPM/ASTRO on image guided technologies

J. De Los Santos et al. " Iimage guided radiation therapy (IGRT) technologies for radiation therapy localization and delivery" IJROBP 87(1) 33-45; 2013

Site specific Inter and intra fraction mobility

- Site-specific goals and uncertainties
- Dosimetric consequences of exceeding tolerances
- Desirable IGRT characteristics and feasible systems to achieve goals
- IGRT process designs to minimize site-specific uncertainties
- Sites used as examples of critical thinking process in this presentation: lung, liver, prostate, spine SBRT, H&N

University of Virginia Health System

UNIVERSITY of VIRGINIA HEALTH SYSTEM

Intra-fractional uncertainty of Pulmonary tumors with SBRT Tx

- Stereotactic body frame
- Motion of bony anatomy used as a surrogate for patient motion
- 1 -3 fractions lung SBRT, 27 lung lesions
- CBCT pre and post Tx – change in motion envelope
- Bony anatomy is a poor surrogate for tumor position

Table 2
Intra-fractional stability of patient and tumor position

	Mean	SD	90th percentile	Max. error		Mean	SD	90th percentile	Max. error
Patient motion (mm)									
SI	−0.1	1.3	2.2	5.9	3D	2.1	1.4	3.8	7.8
AP	−0.5	1.3	2.2	5.5					
LR	−0.1	1.7	3	7.5					
Absolute tumor drift (mm)									
SI	0.6	1.5	2.7	5.8	3D	2.8	1.6	4.8	7.2
AP	−1.3	1.9	3.6	5.8					
LR	0.3	1.6	2.7	6.8					
Tumor drift rel. to bony anatomy (mm)									
SI	0.7	1.7	2.8	6.6	3D	2.3	1.6	4.4	7.4
AP	−0.8	1.7	3.1	6.4					
LR	0.4	1.0	1.8	3.9					

Mean, standard deviation (SD) maximum and 90th percentile of errors; SI (superior inferior); AP (anterior posterior); LR (left right).

M. Guckenberger et al. " Intra-fractional uncertainties in cone-beam CT based image-guided radiotherapy (IGRT) of Pulmonary tumors" Radiotherapy Oncology 83 (2007) 57-64

Respiratory Motion of Pulmonary Tumors

(a) (b) (c)

Underberg RWM et al IJROBP 2005; 63:253-260

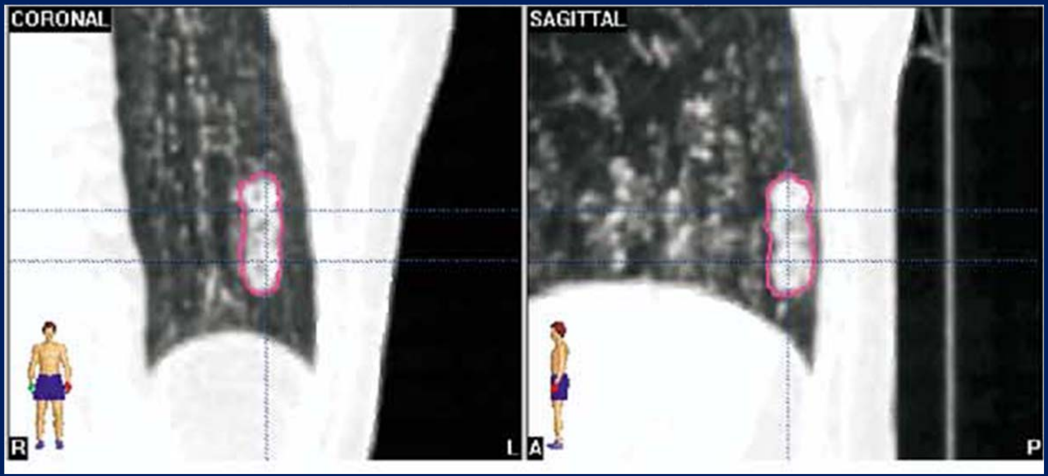

Liu HH et al IJROBP 2007; 68: 531-540 – 152 patients

- Up to 3cm inferior motion
- 95% of lung tumors move <1.3cm I/S, <0.4cm L/R, and <0.6cm A/P
- Tumor motion is highly correlated with diaphragm motion and tumor location in S/I

Lung tumor motion with free breathing- hysteresis

Different path taken during inhalation and exhalation

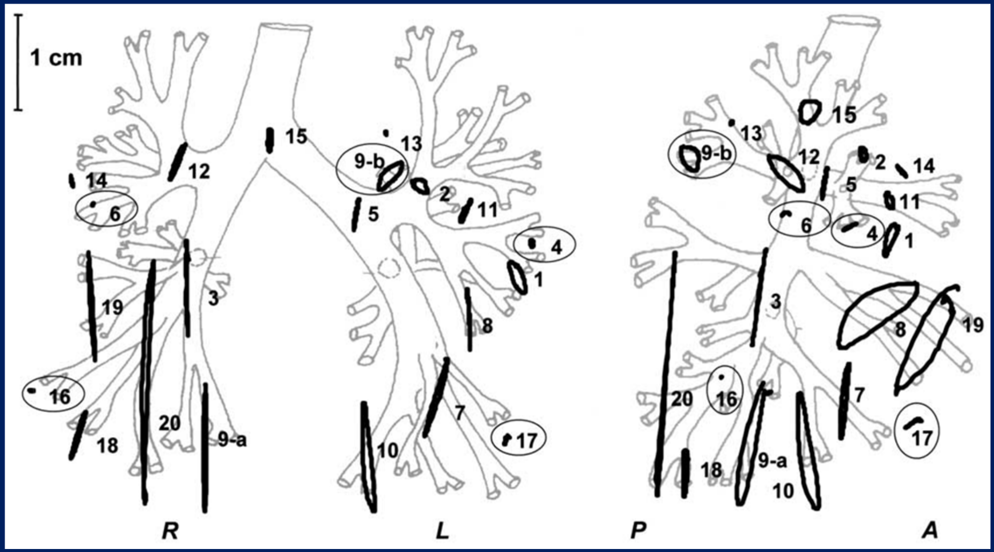

1- 5mm hysteresis of breathing trajectories measured

Seppenwoolde Y. et al. "Precise and real-time measurement of 3D tumor motion in lung due to breathing and heartbeat measured during radiotherapy" IJROBP 2002; 53:822-834

University of Virginia Health System

Comparison of breath hold CBCT and Free breathing CBCT

Figure 1 Digital tomosynthesis image (top) acquired using a breath-held acquisition over 44°, requiring a 7-second breath hold. The improvement in quality over a free-breathing cone- beam CT image (bottom) is because of the lack of breathing-induced movement over the short time of data acquisition. (Courtesy of F.F. Yin, Duke University).

J.M. Balter, Y. Cao "Advanced Technologies in Image-Guided radiation therapy", Seminars in Radiation Oncology 17: 293-297: 2007

Change in volume and position of adenocarcinoma of right lung during radiotherapy

GTV changes from original CT scan (A), to repeat CT scan on day 24 (B), MVCT scan from Tomotherapy on day 60 ©, kVCT scan on day 67 (D)

Gating and real-time tracking to improve pulmonary accuracy of SBRT

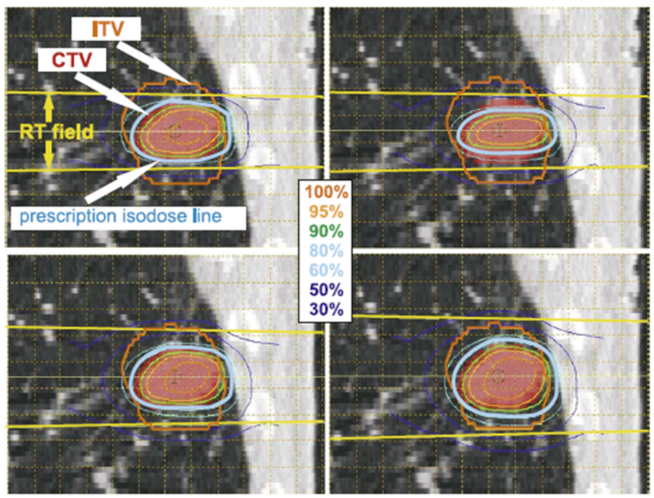

Fig. 1. Four-dimensional treatment planning for compensation of breathing-induced tumor motion (lesion #13); left upper image: 3D treatment planning with the target in mid-ventilation position assuming no breathing motion; the CTV is covered by the 80% isodose; right upper image: 4D dose calculation without additional safety margins for compensation of breathing motion; CTV coverage by the 80% isodose is compromised; left lower image: 4D treatment planning with complete dosimetric motion compensation; the CTV is covered by the 80% isodose; right lower image: 4D dose calculation with geometrical motion compensation; motion is over-compensated with the CTV covered by the 90% isodose in cranio–caudal direction and increased doses to the surrounding pulmonary tissue.

Results: Because of large inter-fractional base-line shifts of the tumor, stereotactic patient positioning and image-guidance based on the bony anatomy required safety margins of 12 mm and 9 mm, respectively. Four-dimensional image-guidance targeting the tumor itself and intra-fractional tumor tracking reduced margins to <5 mm and <3 mm, respectively. Additional safety margins are required to compensate for breathing motion. A quadratic relationship between tumor motion and margins for motion compensation was observed: safety margins of 2.4 mm and 6 mm were calculated for compensation of 10 mm and 20 mm motion amplitudes in cranio–caudal direction, respectively.
Conclusion: Four-dimensional image-guidance with pre-treatment verification of the target position and online correction of errors reduced safety margins most effectively in pulmonary SBRT.

M. Guckenberger, T. Krieger, et al. "Potential of image-guidance, gating and real-time tracking to improve accuracy in pulmonary stereotactic body radiotherapy", Radiotherapy Oncology 19: 288-295: 2009

Lung

– Site-specific goals and uncertainties (e.g. periodic breathing motion, need soft tissue visualization)
– Desirable IGRT characteristics (e.g. soft tissue visualization, ability to assess if breathing motion similar to time of sim → CBCT)
– IGRT Process Decisions (e.g. Transfer ITV for matching to ensure motion-averaged CBCT target aligns within ITV)

Liver motion with free breathing

- Intra-fraction liver motion – 3-18 mm in CC dimension

Case. R. et al "Interfraction and intrafraction changes in amplitude of breathing motion in stereotactic liver radiotherapy ", IJROBP 77 (3): 918- 925: 2010

- Inserted fiducial marker motion has shown Intra fraction liver tumor motion
  - ML direction ~ 1 -12 mm
  - CC direction ~ 2 -19 mm
  - Ap direction ~ 2 – 12 mm

Kitamura, K. , Shirato, H., Seppenwoolde Y. et al "Tumor location, cirrhosis, and surgical history contribute to tumor movement in the liver, as measured during stereotactic irradiation using a real-time tumor-tracking radiotherapy system", IJROBP 56: 221 -228: 2003

Liver motion with free breathing

- The tumor motion of the left lobe was significantly less than that of the right lobe in the LR (2± 1 vs 5 ± 4 mm, p = 0.01) and AP (3 ± 2 vs. 6 ± 3 mm, p = 0.01) directions.
- The tumor motion of the patients with liver cirrhosis was significantly greater than that of the patients without liver cirrhosis in the LR (7 ± 4 vs. 2 ± 1 mm, p = 0.0008) and AP (7 ± 3 vs. 3 ± 2 mm, p = 0.004) directions.
- The tumor motion of the patients who had received partial hepatectomy was significantly less than that of those who had no history of any operation on the liver in the LR (5 ± 4 vs. 2 ± 1 mm, p = 0.04) and AP (6 ± 3 vs. 3 ± 2 mm, p = 0.03) directions.

Kitamura, K. , Shirato, H., Seppenwoolde Y. et al "Tumor location, cirrhosis, and surgical history contribute to tumor movement in the liver, as measured during stereotactic irradiation using a real-time tumor-tracking radiotherapy system", IJROBP 56: 221 -228: 2003

UNIVERSITY of VIRGINIA HEALTH SYSTEM

Liver motion with free breathing- hysteresis

Different path taken during inhalation and exhalation

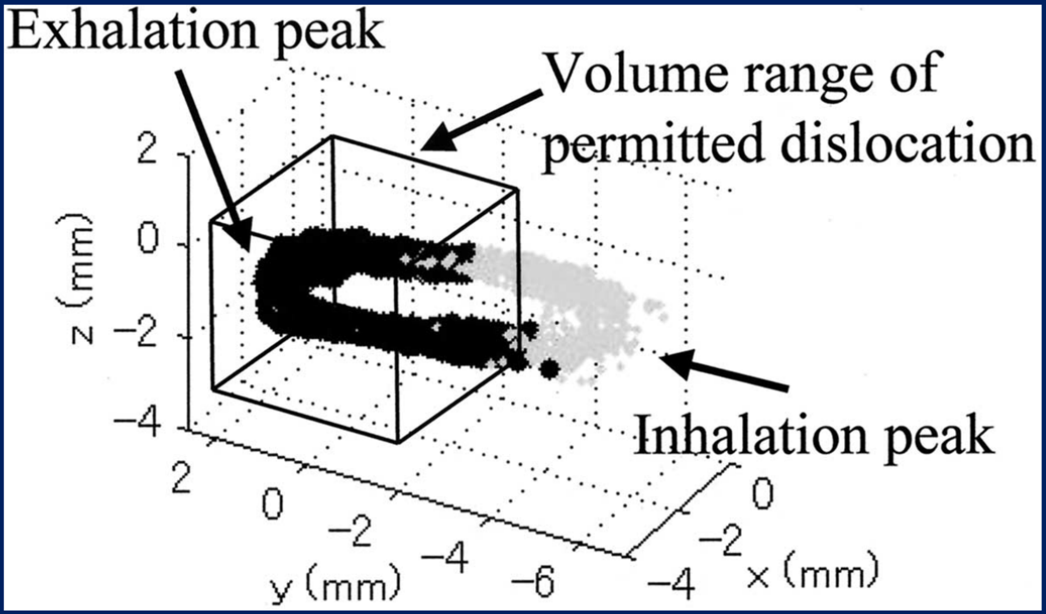

3D path of tumor during beam delivery for a single day. Black dots represent irradiated tumor position; gray dots represent nonirradiated tumor position every 0.09 s. Permitted dislocation shown as a 2-mm box around the exhalation peak. x, LR; y, CC; and z, AP.

Kitamura, K. , Shirato, H., Seppenwoolde Y. et al “Tumor location, cirrhosis, and surgical history contribute to tumor movement in the liver, as measured during stereotactic irradiation using a real-time tumor-tracking radiotherapy system”, IJROBP 56: 221 -228: 2003

Measurements of Abdominal Tumor Motion

Bradner GS et al IJROBP 2006; 65: 554-560 – 13 patients

- Up to 2.5cm inferiorly for all tumors, motion up to 1.2 cm A/P observed for liver and kidneys
- Mean S/I displacements: Liver 1.3cm; Spleen 1.3 cm; Kidneys 1.2cm

Liver motion with breath hold (ABC) and intra-arterial microcoils

- Intra-fraction liver motion in CC dimension
  - 2.5 mm (range 1.8 –3.7 mm) -diaphragm
  - 2.3 mm (range 1.2–3.7 mm) – hepatic microcoils
- Inter-fraction liver motion in CC dimension
  - 4.4 mm (range 3.0–6.1 mm) -diaphragm
  - 4.3 mm (range 3.1–5.7 mm)- hepatic microcoils

Need daily on-line imaging and repositioning if treatment margins smaller than those required for free breathing are a goal.

Dawson, LA, Brock,KK et. al. "The reproducibility of organ position using active breathing control (ABC) during liver radiotherapy", IJROBP 51; 1410-21 (2001)

Intra-fraction reproducibility of liver with ABC breath hold

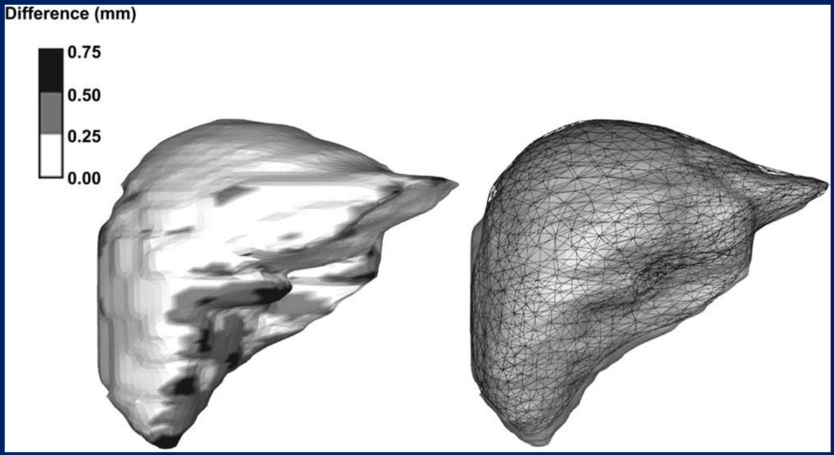

breath-hold computed tomography (CT) scans at the time of simulation. On the left, the liver from the second CT is registered to the liver from the first CT scan using a finite element mesh-based deformable registration tool. The gray scale shows the absolute difference in the position of the liver surfaces. White represents differences within 2.5 mm, whereas black representing differences of 5–7.5 mm. On the right, the first CT is shown in solid and the second is shown in wire frame.

Eccles C., Brock K.K. et. al. “Reproducibility of liver position using active breathing coordinator for liver cancer radiotherapy”, IJROBP 64 (3); 751-759 (2006)

Liver motion with DIBH for obese patients

- The mean of the absolute value of liver shift between daily CBCT acquisitions and planning DIBH CT was
  - AP -2.6 mm (SD 1.7 mm)
  - Lat -3.5 mm (SD 1.8 mm)
  - Sup/Inf 4.4 mm (SD 1.9 mm)
- The mean 3-D deviations for the patients who received paracenteses for ascites was 2.3 mm (95% CI: 0.7-3.9 mm) and 1.6 mm (95% CI: 0.7-2.5 mm) for those who did not

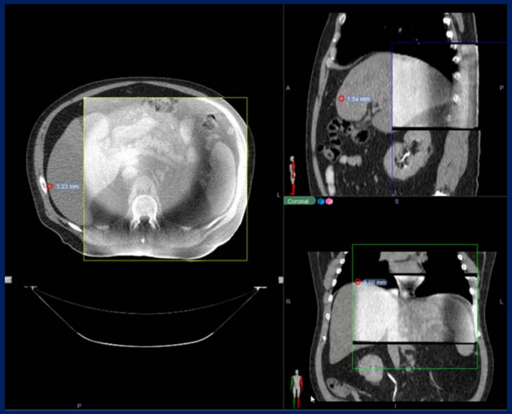

Sunil W. Dutta et. al. "Assessing inter and intra-fraction liver motion during radiotherapy in patients with obesity or ascites (ASTRO 2017)

Liver

- – Site-specific goals and uncertainties (e.g. low contrast target, periodic breathing motion)
- – Desirable IGRT characteristics (e.g. minimize breathing motion to optimize ability to visualize low contrast targets, multiple fiducial markers inside target)
- – IGRT Process Decisions (e.g. breath-hold treatment if possible, use of PRV to allow for OAR inter-fx motion on day of treat)

University of Virginia Health System

Intra-fraction prostate motion measured by Calypso system

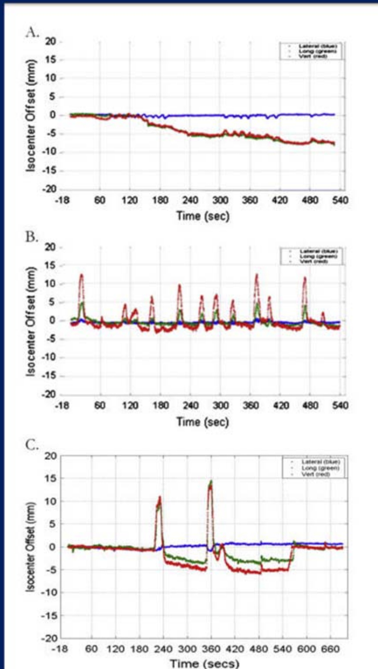

Fig. 1. (A) Drift motion. (B) Transient motion. (C) Drift and transient motion. The track shown in (C) shows an incident when therapists intervened and corrected couch position in response to observed motion (at time, 560 s). For data analysis purposes, these couch corrections were retrospectively eliminated by reintroducing the offset that had been corrected by therapists.

← Sustained Excursion

Prostate drifts from isocenter

Longitudinal and vertical posterior motion

RT(T) shifts table during treatment

High Frequency, Transient Excursion →

Prostate shifts erratically – 9 minutes

15% of patients exhibit prostate movement >5mm from initial position within 10s mainly in S/I direction

Left-Right motion is the least

Kupelian et al "Multi-institutional clinical experience with the Calypso system in localization and continuous real-time monitoring of the prostate gland during external radiotherapy", IJROBP 67: 1088-1098: 2007

Langen et al "Observations on real-time prostate gland motion using electromagnetic tracking", IJROBP 71: 1084-1090: 2008

Inter/Intra-fraction prostate motion measured by Varian OBI system and internal gold markers

a) Typical example of inter-fraction displacement where gold marker displacement relative to bony anatomy in AP kV images at different fractions
b) Example of intra-fraction displacements where the gold marker moves >2mm in the S/I direction after 2min

B. Sorcini et al "Clinical application of image-guided radiotherapy, IGRT (on the Varian OBI platform)", Cancer Radiotherapy 10: 252-257: 2006

Compare fiducials to prostate guidance

- Little difference between fiducial markers to prostate in CBCT
- Difference in residual error 1.1mm (SD 2.9)

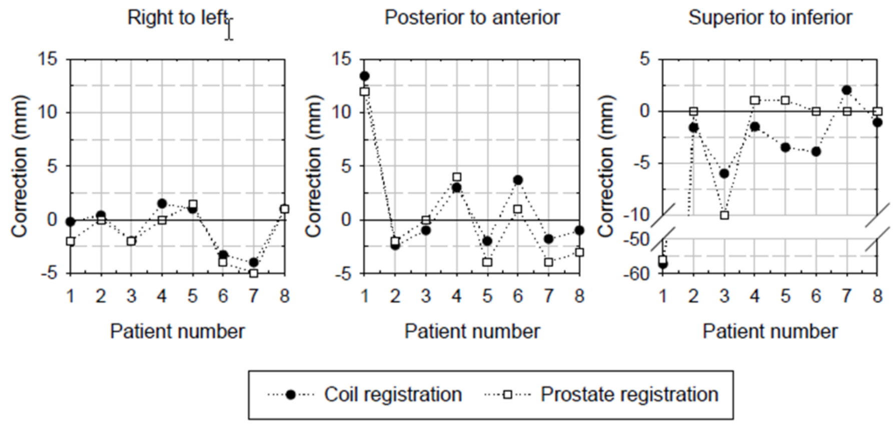

Fig. 6. Comparison of setup corrections obtained by fusing first x-ray volumetric imaging (XVI) data set to planning computed tomography (CT) scan using soft-tissue (contour-to-contour) and marker registration methods.

Letourneau D et al "Assessment of residual error for online cone-beam Ct guided treatment of prostate cancer patients", IJROBP 62: 1239-46: 2005

Prostate Motion in Obese Men

Table 1. Absolute daily patient positioning error

	SI (mm)	LR (mm)	AP (mm)
Mean	7.2	11.4	2.6
Median	5	8	2.5
Range	0–47	0–42	0–8
95% CI	5.3–9.1	9.0–13.8	1.8–3.3

Abbreviations: SI = superior/inferior; LR = left/right; AP = anteroposterior; CI = confidence interval.

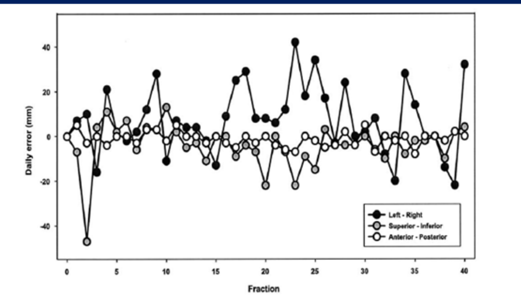

Fig. 3. Magnitude and direction of daily positioning error in 1 patient as an example of the variation in daily setup of an obese patient. Bony landmarks were used to determine setup error for fractions 1–25. Gold seeds were used to determine patient positioning error for fractions 26–40 combining organ motion and setup error into one numerical value.

Left-Right motion is the largest in Obese men >10mm !

LE Millender et al "Daily electronic portal imaging for morbidly obese men undergoing radiotherapy for localized prostate cancer", IJROBP 59 (1): 6-10: 2004

Prostate Motion in Obese Men

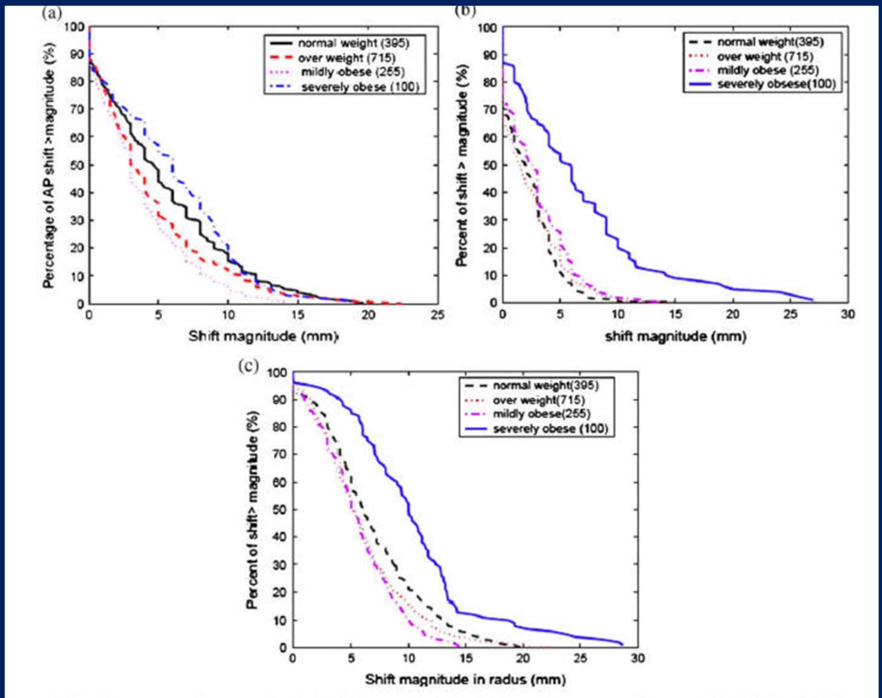

Fig. 3. (a) Percent anterior–posterior (AP) shift in magnitude for the four patient groups. (b) Percent left–right (LR) shift in magnitude for the four patient groups. (c) Percent radius shift in magnitude for the four patient groups.

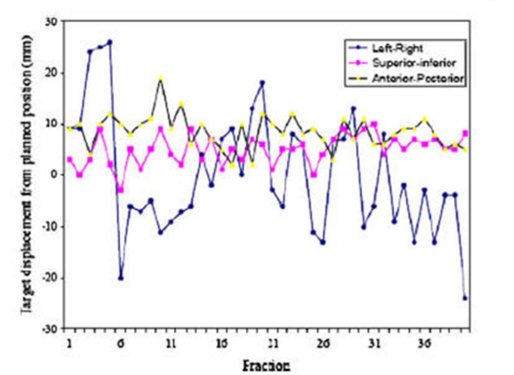

Fig. 7. Daily prostate shifts measured for a patient weighing 450 lb (see text for details).

JR Wong et al "Potential for higher treatment failure in obese patients: correlation of elevated body mass index and increased daily prostate deviations from the radiation beam isocenters in an analysis of 1,465 CT images", IJROBP 75: 49-55: 2009

Dosimetric consequences of prostate motion

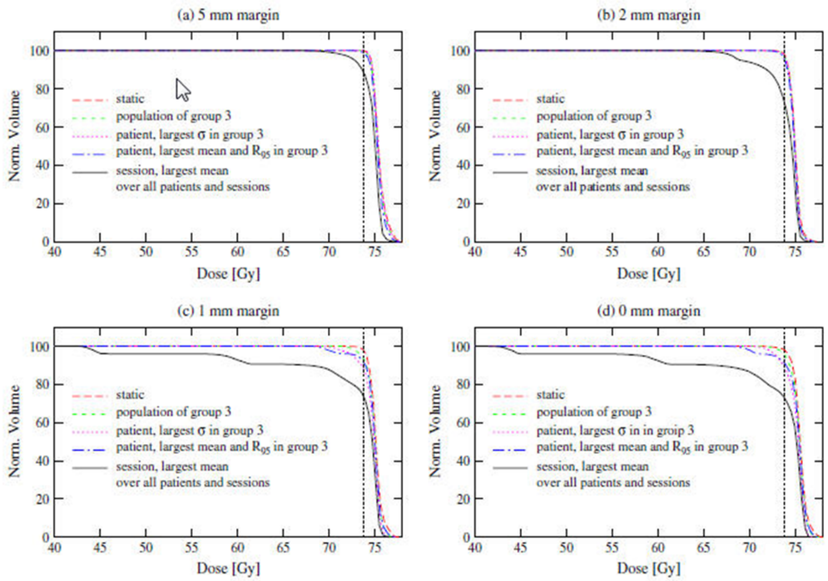

Fig. 7. Prostate dose–volume histograms (DVHs) for different prostate–planning target volume (PTV) margins for the static and motion-convolved plans in different scenarios: the average for the patient population in Group 3 (no interruptions), the patient with the largest SD in Group 3, the patient with the largest mean (who also showed the largest R_{95} amplitude) in Group 3, and the individual session with the largest mean motion for all patients and sessions. Note that with 2- and 5-mm margins, DVHs are indistinguishable from one another, with the exception of the single session with the largest motion. R_{95} = amplitude that accommodates the motion for 95% of the tracking time.

- HS Li et al “Dosimetric consequences of intra-fraction prostate motion”, IJROBP 71: 801-812: 2008

Dosimetric consequences of prostate motion

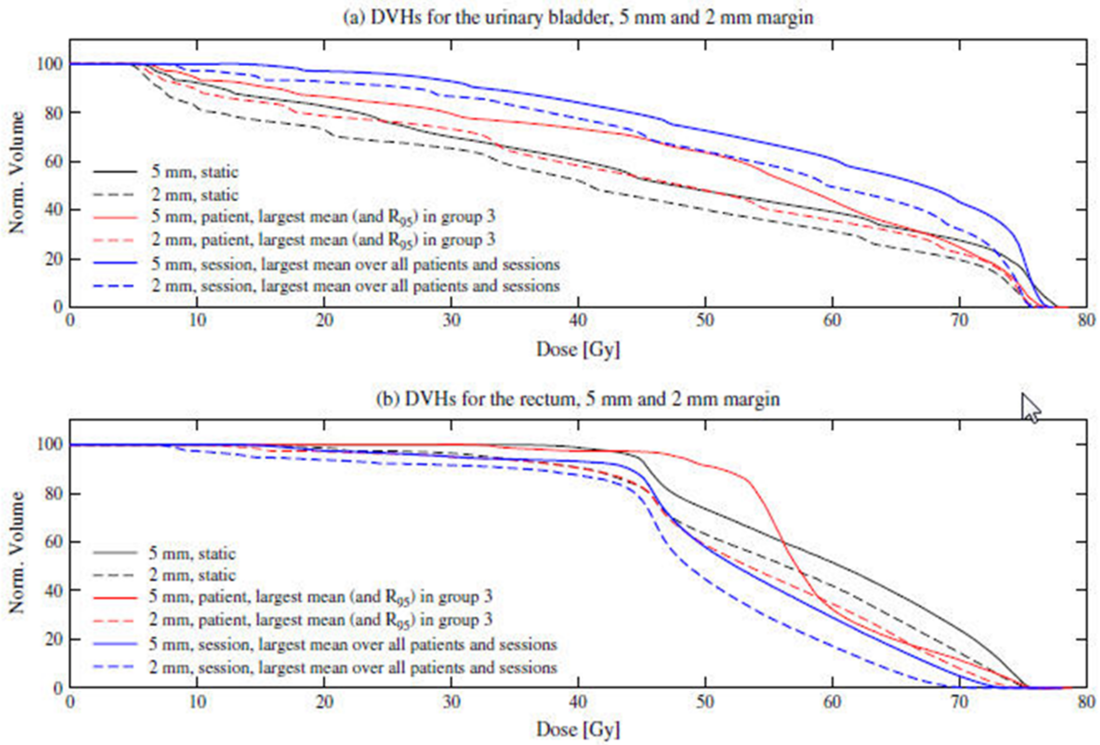

Fig. 8. Dose–volume histograms (DVHs) for (a) the bladder and (b) rectum with 2- and 5-mm prostate–planning target volume (PTV) margins for the static and convolved plan for the motions scenarios: the patient with the largest mean value (who also showed the largest R_{95} amplitude) in Group 3, and the individual session with the largest mean motion for all patients and sessions. R_{95} = amplitude that accommodates the motion for 95% of the tracking time.

- HS Li et al “Dosimetric consequences of intra-fraction prostate motion”, IJROBP 71: 801-812: 2008

Clinical impact of prostate motion in Obese Men

Probability of 10-year biochemical failure-free survival after EBRT for obese patients is:
20-25% lower than that for the normal weight
62-65% lower than for mildly obese patient group

- Strom et al “Influence of obesity on biochemical and clinical failure after external-beam radiotherapy for localized prostate cancer”, Cancer 107: 631-639: 2006

Prostate

– Site-specific goals and uncertainties (e.g. discrete and unpredictable target motion)
– Desirable IGRT characteristics (e.g. soft tissue visualization, periodic intra-fx verification)
– IGRT Process Decisions (e.g. tradeoffs and clinical use of CBCT and OBI-fiducial-based imaging)

Intra-Fraction Motion of Spine During SBRT

3.3 mm –Using a stereotactic body frame

Shiu AS, Chang AL, et al. “Near simultaneous computed tomography image guided stereotactic spine radiotherapy: an emerging paradigm for achieving true stereotaxy” IJROBP 57: 605-613 (2013)

5.2 mm – using whole body vaccum cushion

Yanice kM,Lovelock DM, et al. “CT image guided intensity odulated radiation therapy for paraspinal tumors using stereotactic immobilization”, IJROBP 55: 583-593 (2003)

Table 2
Patient set-up errors

	M	Σ	σ	max
Translational errors (mm)				
SI	−0.3	2.0	3.8	11
AP	0.5	1.2	2.4	11
LR	0.6	2.1	3.0	15
Rotational error (°)				
SI	−0.3	1.4	1.3	8
AP	−0.6	1.2	1.4	7
LR	0	1.3	1.4	6

Set-up errors observed during treatment. Reported are group mean errors (M), distribution of systematic (Σ) and of random (σ) positioning errors.

Mathias Guckenberger al “Precision required for dose-escalated treatment of spinal metastases and implications for image-guided radiation therapy (IGRT)”, Radiotherapy Oncology 84: 56 -63: 2007

UNIVERSITY of VIRGINIA HEALTH SYSTEM

Precision Requirements for Spine SBRT –Dosimetric consequences

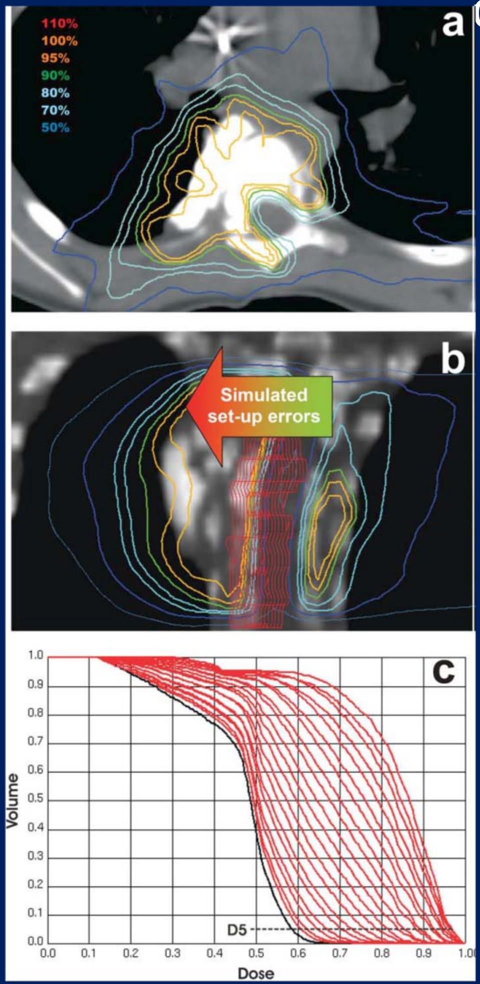

a) Dose distribution in the axial plane
b) Simulated transversal patient set-up errors (0.5-1.00mm) with resulting displacements of the spinal cord
c) Dose to the spinal cord:
   - Black – prescribed dose from Tx plan
   - Red – dose distributions resulting from simulated set up errors

To keep dose to spinal cord within ± 5% (± 10%) of the Rx dose maximum errors should be within

1mm (2mm)- transverse
4mm (7mm) – S/I
3.5 deg (5 deg) - rotations

Mathias Guckenberger al "Precision required for dose-escalated treatment of spinal metastases and implications for image-guided radiation therapy (IGRT)", Radiotherapy Oncology 84: 56 -63: 2007

University of Virginia Health System

Precision Requirements for Spine SBRT

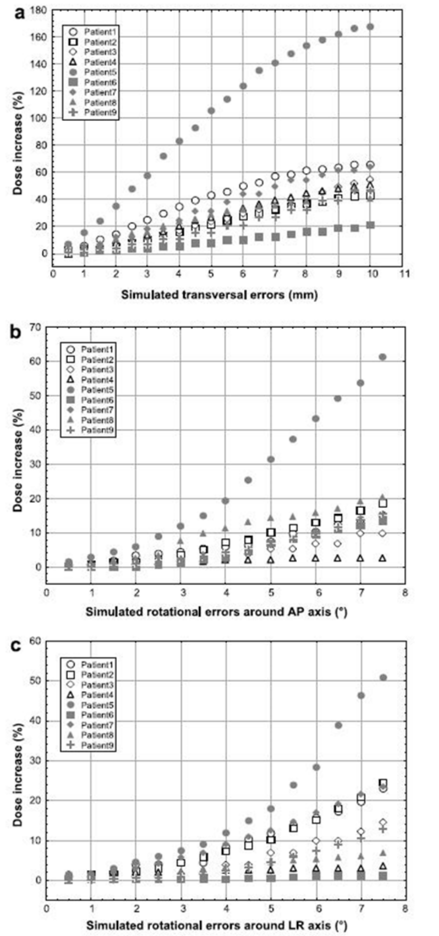

Fig. 2. Simulation of patient set-up errors and influence of these displacements on the dose to the spinal cord $D5^{spine}$ (dose relative to the planned dose). (a) Simulation of transversal set-up errors from 0.5 to 10 mm. (b) Simulat axis from 0.5° to 7.5°. (c) Simu LR axis from 0.5° to 7.5°.

Translational errors in the transverse plane has the dominant effect on $D5^{spine}$

3mm → 18 ± 16%
5mm → 34 ± 29%
7mm → 48 ± 34%

Translational errors in the S/I direction effect on $D5^{spine}$

3mm → 1 ± 2%
5mm → 6 ± 3%
7mm → 9 ± 5%

Rotational errors in the A/P axis and L/R axis effect on $D5^{spine}$

3 deg → 4 ± 3%
5 deg → 9± 7%
7 deg → 16 ± 14%

Clinically observed translational and rotational components of set-up errors increased D5 _cord by an average of:

23±14%, and 3±2%

Mathias Guckenberger al "Precision required for dose-escalated treatment of spinal metastases and implications for image-guided radiation therapy (IGRT)", Radiotherapy Oncology 84: 56 -63: 2007

Spine SBRT

- Site-specific goals and uncertainties (e.g. very tight margins, rotations very important, no periodic motion, but intra-fraction motion high risk)
- Desirable IGRT characteristics (e.g. CBCT good for 3D visualization of target and OARs)
    - Dosimetric consequences of intra- and inter-fraction setup errors in Spine SBRT.
- IGRT Process Decisions (e.g. mid-treatment verification imaging to reduce likelihood of intra-fx)

Dosimetric effects due to weight loss during RT

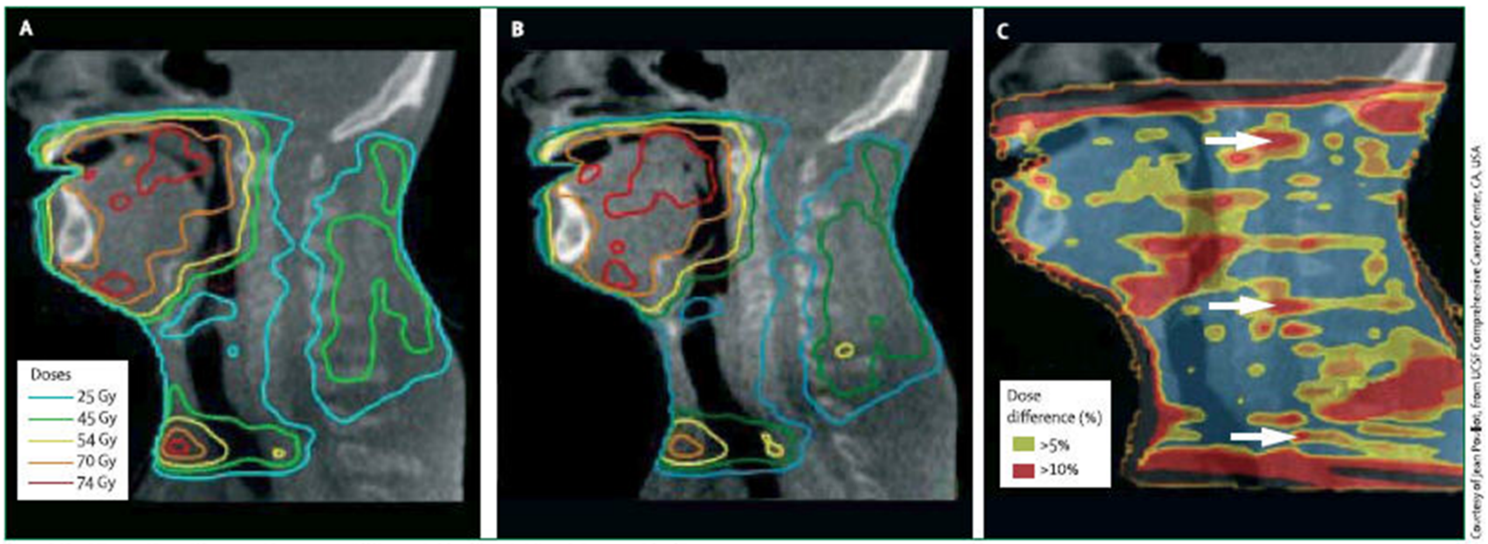

Figure 6: **Differing doses because of anatomical changes from weight loss during radiotherapy**
Substantial anatomical changes between weeks 1 (A) and 3 (B) detected on megavoltage cone-beam CT scans (figure 5) result in a change in delivered dose. In dose-difference image (C), arrows=locations in spinal cord that received 10% or more dose than planned.

>10% dose differences in dose to code shown in arrows

H&N IMRT

– Site-specific goals and uncertainties (e.g. complex dose distributions adjacent to many critical structures, and sensitive to rotations due to long target)
– Desirable IGRT characteristics (e.g.soft tissue visualization and ability to detect rotations)
– IGRT Process Decisions (e.g. may use OBI for daily setup and CBCT weekly to assess if replan needed)

University of Virginia Health System

Correction stratergies for setup errors Adaptive RT

- Online procedures – tumor is in close proximity to critical structures or high dose RT
  - Acquires images daily
  - Assesses info from daily imaging prior to Tx
  - Simple corrections implemented to compensate noted deviations in position
  - Larger reduction in geometric errors than offline approaches
- Offline procedures -
  - frequent acquisition of images without immediate intervention
  - Calculate systematic and random uncertainties of set up error
  - Correction for systematic error made for the remaining fractions

Adaptive Rt –

Replanning before every tx based on 3D image acquired

Replan only when substantial changes to anatomy is observed

Time lag between image acquisition and decision to enable/disable beam

- 0.03 seconds is fast enough to maintain target position within 1mm of predicted for motions with speeds up to 3.3 cm/s
- The issues of lag and dose suggest we would benefit from combining internal and external guidance – Cyberknife uses implanted markers and periodic radiography, but uses an external coordinate to estimate the internal position

J.M. Balter, Y. Cao “Advanced Technologies in Image-Guided radiation therapy”, Seminars in Radiation Oncology 17: 293-297: 2007

Daily variation of prostate location with respect to bony anatomy

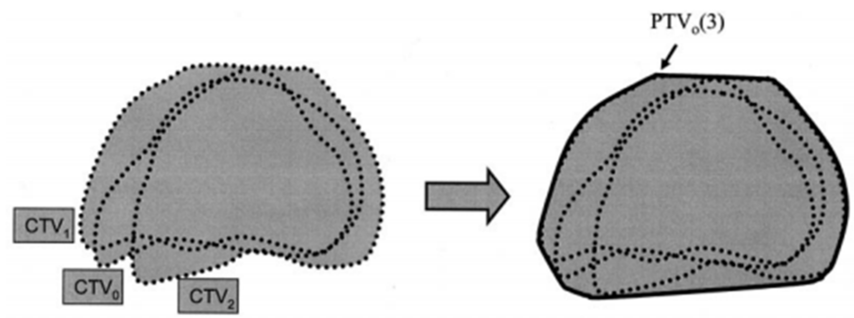

Fig. 1. Illustration of the convex hull of multiple clinical target volumes (CTVs) and planning target volume (PTV).

Online correction stratergy: Pre-Tx imaging and align to soft tissue
Can also create a bounding box from first k days of daily CTVs – Advantage: eliminate the effects of systematic variation in internal target location

Yan D., Lockman D, et. al. "An offline strategy for constructing a patient- specific planning target volume in adaptive treatment process for prostate cancer", IJROBP 48 (1); 289-302 (2000)

Substantial anatomical change due to weight loss during RT

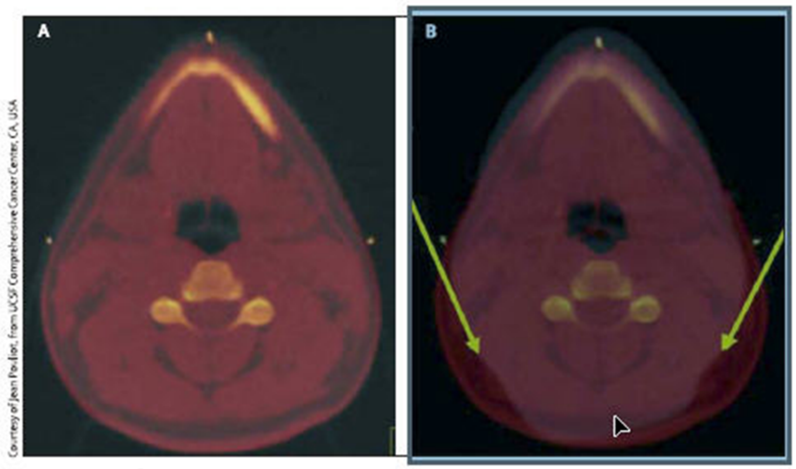

Figure 5: **Megavoltage cone-beam CT scans of head and neck cancer**
Substantial anatomical change seen between weeks 1 (A) and 3 (B), which is attributable to weight loss during radiotherapy (highlighted with yellow arrows).

Offline correction strategy: re-simming and re-planning

Summary

- IGRT tolerances and techniques depend on the Tx site, dose fractionation, nearby critical structure doses, and also patient size/immobilization
- If used inappropriately, will lead to unsuitable margin reduction, and missing the tumor
- At present IGRT does not measure biological change/healthy tissue function
- Online/offline IGRT both reduce dose delivery to healthy tissue/enable dose escalation
- Allows to adapt radiotherapy to changes in tumor shape/size/location